Numerical investigation of three dimensional viscoelastic free surface flows: impacting drop problem

11th World Congress on Computational Mechanics (WCCM XI)
5th European Conference on Computational Mechanics (ECCM V)
6th European Conference on Computational Fluid Dynamics (ECFD VI)
E. Oñate, J. Oliver and A. Huerta (Eds)

NUMERICAL INVESTIGATION OF THREE DIMENSIONAL VISCOELASTIC FREE SURFACE FLOWS: IMPACTING DROP PROBLEM

RAFAEL A. FIGUEIREDO*, CASSIO M. OISHI†, JOSÉ A. CUMINATO*, JOSÉ C. AZEVEDO⋆, ALEXANDRE M. AFONSO ⋆ AND MANUEL A. ALVES⋆

* Department of Mathematics and Computer Science,
Instituto de Ciências Matemáticas e de Computação (ICMC)
Universidade de São Paulo (USP), São Carlos, Brazil
e-mail: rafigueiredo22@gmail.com, jacumina@icmc.usp.br

† Department of Mathematics and Computer Science,
Universidade Estadual Paulista (UNESP), Presidente Prudente, Brazil
e-mail: cassiooishi@gmail.com

⋆ Departamento de Engenharia Química (CEFT),
Faculdade de Engenharia da Universidade do Porto (FEUP), Porto, Portugal
e-mail: jmca@fe.up.pt, aafonso@fe.up.pt, mmalves@fe.up.pt

Key words: Free surface flows, Viscoelastic models, Numerical simulation, Impacting drop problem

Abstract. This work presents a numerical investigation of three dimensional viscoelastic free surface flows. In particular, using two different numerical methodologies, we have simulated a typical free-surface benchmark flow problem: the impact of a viscoelastic fluid droplet with a rigid boundary. The numerical method was recently proposed by Figueiredo et al. [1] and has been implemented in a in-house viscoelastic flow solver. In this methodology, a finite difference scheme is adopted combining the Marker-And-Cell (MAC) method with a Front-Tracking strategy. In order to preserve mass conservation properties for transient viscoelastic fluid flows, we have modified the methodology in [1] to include an improvement on the MAC discretization of the velocity boundary conditions at free-surfaces. The code is verified by solving the drop impact problem for a Newtonian fluid. After this verification, we employ the Oldroyd-B model to assess the differences between the methodologies, and compare our results with the ones in the literature. Finally, a detailed study of the influence of the relevant rheological parameters of the non-linear viscoelastic models (Giesekus and XPP) is reported, regarding the deformation and spreading of the viscoelastic fluid drop after impacting on a rigid surface.

1 INTRODUCTION

In computational rheology, one interesting challenge is to produce an accurate method for solving viscoelastic fluid flows in the presence of free surface boundary conditions. Due to the hyperbolic character of the constitutive equation defining the fluid model and the large deformations caused by the moving interface, several authors have proposed numerical modifications to traditional numerical approaches (e.g. [2, 3, 4]).

A typical three-dimensional benchmark problem in computational rheology involving free surfaces and viscoelastic models is the impact of a fluid droplet onto a rigid boundary (see Figure 1). In this flow problem, a spherical drop falls under the action of gravity until it impacts a solid surface. From a rheological point-of-view, a peculiar behaviour appears in the simulation after the impact since the viscoelastic fluid drop undergoes deformations due to shear and elongational deformations which are influenced by rheological properties of the fluid.

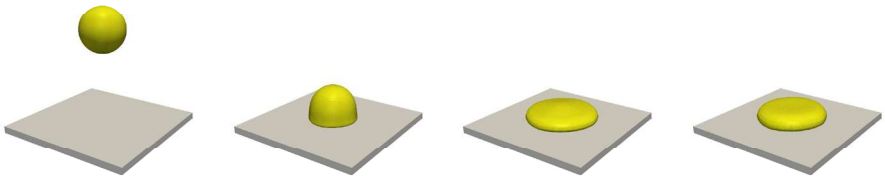

Figure 1: Illustration of the numerical simulation of the impacting drop problem.

The impact drop problem has been widely studied using numerical methods in two dimensions [5, 6, 7, 4]. However, for three dimensional simulations and viscoelastic models, there are few papers [8, 9] dealing with impacting and spreading of a viscoelastic drop on a horizontal surface.

Therefore, this work tries fill this gap by presenting a numerical investigating of the impact drop problem in three-dimensions for a viscoelastic fluid model. In order to improve the combination of the front-tracking method with the MAC formulation, we have proposed a modification in the interpolation of the velocities at free surface. This modification has been implemented in our three dimensional viscoelastic code [1]. We intend that the results of this work be useful both; for testing numerical methods and for promoting the understanding of the rheological behaviour of polymers in flows with industrial relevance.

2 GOVERNING EQUATIONS

Incompressible, viscoelastic and isothermal flows can be modelled by the following system of partial differential equations:

- the mass conservation equation

$$\nabla \cdot \mathbf{u} = 0, \tag{1}$$

- the momentum balance

$$\frac{\partial \mathbf{u}}{\partial t} + \nabla \cdot (\mathbf{uu}) = -\nabla p + \frac{\beta}{Re}\nabla^2 \mathbf{u} + \nabla \cdot \boldsymbol{\tau} + \frac{1}{Fr^2}\mathbf{g}, \tag{2}$$

- the constitutive equation

$$\frac{\partial \boldsymbol{\tau}}{\partial t} + \nabla \cdot (\mathbf{u}\boldsymbol{\tau}) - \left[(\nabla \mathbf{u}) \cdot \boldsymbol{\tau} + \boldsymbol{\tau} \cdot (\nabla \mathbf{u})^{\mathbf{T}}\right] = F(\boldsymbol{\tau}), \tag{3}$$

where t is time, $\mathbf{u}$ is the velocity vector field, p is the pressure and $\mathbf{g}$ is the gravity field. In Eq. (2), $\boldsymbol{\tau}$ is the non-Newtonian part of the extra-stress tensor which is defined by Eq. (3). The term on the right hand side of the Eq. (3) defines the viscoelastic fluid model, where

$$F(\boldsymbol{\tau}) = \begin{cases} 2\xi \mathbf{D} - \dfrac{1}{Wi}\boldsymbol{\tau} & \text{Oldroyd-B,} \\ 2\xi \mathbf{D} - \dfrac{1}{Wi}\left[\boldsymbol{\tau} + \dfrac{\alpha}{\xi}\boldsymbol{\tau} \cdot \boldsymbol{\tau}\right] & \text{Giesekus,} \\ 2\xi \mathbf{D} - \dfrac{1}{Wi}\left\{f(\lambda, \boldsymbol{\tau})\boldsymbol{\tau} + \xi\left[f(\lambda, \boldsymbol{\tau}) - 1\right]\mathbf{I} + \dfrac{\alpha}{\xi}\boldsymbol{\tau} \cdot \boldsymbol{\tau}\right\} & \text{XPP,} \end{cases} \tag{4}$$

with

$$f(\lambda, \boldsymbol{\tau}) = \frac{2}{\gamma}\left(1 - \frac{1}{\lambda}\right) e^{Q_o(\lambda - 1)} + \frac{1}{\lambda^2}\left[1 - \frac{\alpha}{3\xi^2} tr(\boldsymbol{\tau} \cdot \boldsymbol{\tau})\right], \tag{5}$$

$$\lambda = \sqrt{1 + \frac{1}{3\xi} tr(\boldsymbol{\tau})}. \tag{6}$$

The dimensionless parameters $Re = \frac{\rho L U}{\mu}$, $Fr = \frac{U}{\sqrt{gL}}$ and $Wi = \frac{\lambda_1 U}{L}$ are the Reynolds, Froude and Weissenberg numbers, respectively, where L and U are length and velocity scales, ρ is the density, μ is the total viscosity (sum of the polymeric viscosity coefficient μ_p and solvent viscosity μ_s) and λ_1 is the relaxation time of the fluid. The tensor $\mathbf{D} = \frac{1}{2}\left[(\nabla \mathbf{u}) + (\nabla \mathbf{u})^{\mathrm{T}}\right]$ is the rate of deformation tensor. In addition, the viscoelastic parameters are defined as $\beta = \frac{\mu_p}{\mu}$, $\gamma = \frac{\lambda_2}{\lambda_1}$, $\xi = \frac{1-\beta}{ReWi}$ and $Q_0 = \frac{2}{Q}$, where Q is the number of arms at the extremity of the Pom-Pom molecule in the extended Pom-Pom (XPP) model.

The anisotropy parameter, α, controls the influence of the second-normal stress difference and according to [10], α must be set between 0 and 0.5 to ensure physically acceptable results. In particular, for $f(\lambda, \boldsymbol{\tau}) = 1$ the XPP model reduces to the Giesekus model. Furthermore, when $\alpha = 0$ and $f(\lambda, \boldsymbol{\tau}) = 1$ are imposed, the XPP model reduces to the

Oldroyd-B model which is representative of constant shear viscosity viscoelastic fluids, also known as Boger fluids.

A further difficulty arises when the flow involves free surfaces. In this case, an efficient technique to represent the interface in the numerical simulation is required. Among various techniques proposed in the literature we highlight the works of Ville et al. [11] in the simulation of the jet buckling phenomenon by a Level-Set method, Xu et al. [9] in the study of the impact of a viscoelastic drop by a Smoothed Particle Hydrodynamics (SPH) method, and Habla et al. [12] in the analysis of the Weissenberg effect with a Volume of Fluid (VOF) technique.

Recently, Figueiredo et al. [1] have presented a numerical method based in the SMAC method ([13]) for solving three dimensional free surface viscoelastic fluid flows. In the method of Figueiredo et al., following the SMAC formulation, only marker particles are used to represent the free surface. Thus there are two types of meshes: a Lagrangian mesh (representing the fluid interface) and an Eulerian mesh (where the velocities are stored in the faces of cell while other fluid properties are stored in the center of cell). In order to determine the new position of the marker particles, it is necessary to solve the following ODE for each particle:

$$\frac{d\mathbf{x}}{dt} = \mathbf{u}_p, \tag{7}$$

where $\mathbf{u}_p$ is the velocity and $\mathbf{x}$ is the position of the particles. The velocity $\mathbf{u}_p$ is calculated by interpolation from the velocity obtained in the solution of Eq. (2). More details about the SMAC methodology can be found in [14].

3 NUMERICAL METHOD

In this work, we use a finite difference method for solving equations (1)–(3) in a staggered grid. A full description of this scheme can be found in [1]. In addition, an improvement in the interpolation used in the boundary conditions on free surface proposed by [4], will be extended to the three dimensional case.

In summary, using the Crank-Nicolson method, the time discrete approximation for Eq. (2) is written as

$$\frac{\mathbf{u}^{(n+1)} - \mathbf{u}^{(n)}}{\delta t} + \nabla\cdot(\mathbf{uu})^{(n)} + \nabla p^{(n\,|\,1)} = \frac{\beta}{2Re}\left[\nabla^2\mathbf{u}^{(n)} + \nabla^2\mathbf{u}^{(n\,|\,1)}\right] + \nabla\cdot\boldsymbol{\tau}^{(n\,|\,\frac{1}{2})} + \frac{1}{Fr^2}\mathbf{g}, \tag{8}$$

where,

$$\nabla\cdot\boldsymbol{\tau}^{(n+\frac{1}{2})} = \frac{1}{2}\left(\nabla\cdot\widetilde{\boldsymbol{\tau}}^{(n+1)} + \nabla\cdot\boldsymbol{\tau}^{(n)}\right). \tag{9}$$

The tensor $\widetilde{\boldsymbol{\tau}}^{(n+1)}$ is calculated in the process of solution of the Eq. (3) by the second-order Runge-Kutta method

$$\frac{\widetilde{\boldsymbol{\tau}}^{(n+1)} - \boldsymbol{\tau}^{(n)}}{\delta t} = H(\mathbf{u}^{(n)}, \boldsymbol{\tau}^{(n)}) \tag{10}$$

and

$$\frac{\boldsymbol{\tau}^{(n+1)} - \boldsymbol{\tau}^{(n)}}{\delta t} = \frac{1}{2}\left[H(\mathbf{u}^{(n)}, \boldsymbol{\tau}^{(n)}) + H(\mathbf{u}^{(n+1)}, \widetilde{\boldsymbol{\tau}}^{(n+1)})\right], \tag{11}$$

where

$$H(\mathbf{u}, \boldsymbol{\tau}) = F(\boldsymbol{\tau}) - \nabla \cdot (\mathbf{u}\boldsymbol{\tau}) + \left[(\nabla \mathbf{u}) \cdot \boldsymbol{\tau} + \boldsymbol{\tau} \cdot (\nabla \mathbf{u})^{\mathbf{T}}\right]. \tag{12}$$

The velocity and pressure fields are coupled in Eq. (8). To uncouple these fields, the pressure $p^{(n+1)}$ is approximated by $p^{(n)}$ and thus is possible to calculate an intermediate velocity field, $\widetilde{\mathbf{u}}$, from Eq. (8). To obtain an update of the velocity and pressure fields, we apply the projection method [1]. Thus the velocity and pressure fields are calculated as

$$\mathbf{u}^{(n+1)} = \widetilde{\mathbf{u}}^{(n+1)} - \nabla\psi, \tag{13}$$

$$p^{(n+1)} = p^{(n)} + \frac{\psi^{(n+1)}}{\delta t} - \frac{\beta}{2Re}\nabla^2\psi^{(n+1)}, \tag{14}$$

where, ψ is the pressure correction obtained by solving the Poisson equation

$$\nabla^2\psi^{(n+1)} = \nabla \cdot \widetilde{\mathbf{u}}^{(n+1)}, \tag{15}$$

with appropriate boundary conditions (see [1]).

3.1 Boundary condition for the pressure at the free surface

To simulate flows with free surface, it is necessary to impose the boundary conditions for the velocity and pressure at the free surface. In the three-dimensional case there are three conditions:

$$\mathbf{n} \cdot (\sigma \cdot \mathbf{n}^{\mathrm{T}}) = 0, \tag{16}$$

$$\mathbf{t}_i \cdot (\sigma \cdot \mathbf{n}^{\mathrm{T}}) = 0, \quad \text{with} \quad i = 1, 2, \tag{17}$$

where $\mathbf{n} = (n_x, n_y, n_z)$ is the unit normal vector, $\mathbf{t}_i = (t_{ix}, t_{iy}, t_{iz})$ is the unit tangencial vector and $\sigma = -p\mathbf{I} + \frac{2\beta}{Re}\mathbf{D} + \boldsymbol{\tau}$.

According to the methodology described in [1], an implicit strategy to discretize Eq. (17) is essential for obtaining a stable scheme. In summary, a numerical strategy to uncouple velocity and pressure fields in Eq. (17) is proposed, resulting in new equations for the pressure correction, ψ, which are applied at free surface:

$$\frac{\psi^{(n+1)}}{\delta t} - \frac{2\beta}{Re}\left[\left(\frac{\partial^2\psi^{(n+1)}}{\partial y^2} + \frac{\partial^2\psi^{(n+1)}}{\partial z^2}\right)n_x^2 + \left(\frac{\partial^2\psi^{(n+1)}}{\partial x^2} + \frac{\partial^2\psi^{(n+1)}}{\partial z^2}\right)n_y^2\right.$$
$$\left(\frac{\partial^2\psi^{(n+1)}}{\partial x^2} + \frac{\partial^2\psi^{(n+1)}}{\partial y^2}\right)n_z^2 - 2\left(\frac{\partial^2\psi^{(n+1)}}{\partial x\partial y}\right)n_x n_y - 2\left(\frac{\partial^2\psi^{(n+1)}}{\partial x\partial z}\right)n_x n_z$$
$$\left.-2\left(\frac{\partial^2\psi^{(n+1)}}{\partial y\partial z}\right)n_y n_z\right] - \frac{\beta}{2Re}\nabla^2\psi^{(n+1)} = \frac{2\beta}{Re}\left[-\left(\frac{\partial\widetilde{v}^{(n+1)}}{\partial y} + \frac{\partial\widetilde{w}^{(n+1)}}{\partial z}\right)n_x^2\right.$$
$$-\left(\frac{\partial\widetilde{u}^{(n+1)}}{\partial x} + \frac{\partial\widetilde{w}^{(n+1)}}{\partial z}\right)n_y^2 - \left(\frac{\partial\widetilde{u}^{(n+1)}}{\partial x} + \frac{\partial\widetilde{v}^{(n+1)}}{\partial y}\right)n_z^2 \tag{18}$$
$$+\left(\frac{\partial\widetilde{u}^{(n+1)}}{\partial y} + \frac{\partial\widetilde{v}^{(n+1)}}{\partial x}\right)n_x n_y + \left(\frac{\partial\widetilde{u}^{(n+1)}}{\partial z} + \frac{\partial\widetilde{w}^{(n+1)}}{\partial x}\right)n_x n_z$$
$$\left.+\left(\frac{\partial\widetilde{v}^{(n+1)}}{\partial z} + \frac{\partial\widetilde{w}^{(n+1)}}{\partial y}\right)n_y n_z\right] + \left[(\widetilde{\tau}^{xx})^{(n+1)}n_x^2 + (\widetilde{\tau}^{yy})^{(n+1)}n_y^2 + (\widetilde{\tau}^{zz})^{(n+1)}n_z^2\right.$$
$$\left.+2(\widetilde{\tau}^{xy})^{(n+1)}n_x n_y + 2(\widetilde{\tau}^{xz})^{(n+1)}n_x n_z + 2(\widetilde{\tau}^{yz})^{(n+1)}n_y n_z\right] - p^{(n)}.$$

3.2 Improvements in the calculation of the interpolation of the velocities at the free surface

Once the velocity and pressure fields are calculated with the implicit technique, the last step to finalize the computational cycle requires the update of the position of the free surface solving the Eq. (7).

The use of an implicit method to solve the momentum equation for low Reynolds number flows allows the application of a larger time step. According to [7], using an implicity method also requires the use of a stable and accurate scheme for solving Eq. (7). Thus the second order Runge-Kutta method is used

$$\mathbf{x}^{(n+1)} = \mathbf{x}^{(n)} + \frac{\delta t}{2}\left[\mathbf{u}_p\left(\mathbf{x}^{(n)}, t_n\right) + \mathbf{u}_p\left(\widetilde{\mathbf{x}}, t_{n+1}\right)\right], \tag{19}$$

with

$$\widetilde{\mathbf{x}} = \mathbf{x}^{(n)} + \delta t\mathbf{u}_p\left(\mathbf{x}^{(n)}, t_n\right). \tag{20}$$

The proposed improvement in this work extends the ideas of Oishi et al. [4, 7] for the thrcc-dimcnsional casc. Thc vclocity $\mathbf{u}_p$ is calculatcd with bilincar intcrpolation using thc nearest values of the velocities in the Eulerian mesh. However, there are some cases where values of the velocities in Eulerian mesh are not set near the position of the particle. To obtain the values of these velocities a first-order extrapolation is used.

In order to illustrate this extrapolation technique, we consider the case where $\mathbf{n} = \left(-\frac{\sqrt{3}}{3}, \frac{\sqrt{3}}{3}, \frac{\sqrt{3}}{3}\right)$ as shown in Fig. (2). In this figure, the blue cube represents a full cell while the green cubes denotes surface cells. In addition, we illustrate empty cells by red cubes. To interpolate the velocity of the marker particle at the cell i, j, k is required to

obtain the velocities $u_{i-\frac{1}{2},j,k}$, $u_{i-\frac{1}{2},j+1,k}$, $u_{i-\frac{1}{2},j,k+1}$, $v_{i,j+\frac{1}{2},k}$, $v_{i-1,j+\frac{1}{2},k}$, $v_{i,j+\frac{1}{2},k+1}$, $w_{i,j,k+\frac{1}{2}}$, $w_{i-1,j,k+\frac{1}{2}}$ and $w_{i,j+1,k+\frac{1}{2}}$.

The velocities $u_{i-\frac{1}{2},j,k}$, $v_{i,j+\frac{1}{2},k}$ and $w_{i,j,k+\frac{1}{2}}$ must be calculated by Eqs. (1) and (17). One possibility to obtain $u_{i-\frac{1}{2},j+1,k}$, $u_{i-\frac{1}{2},j,k+1}$, $v_{i-1,j+\frac{1}{2},k}$, $v_{i,j+\frac{1}{2},k+1}$, $w_{i-1,j,k+\frac{1}{2}}$ and $w_{i,j+1,k+\frac{1}{2}}$ is to use a zero-order extrapolation. However, in order to maintain accurate mass conservation and accuracy in the calculation of the velocity field at free surface, these velocities can be calculated by a linear extrapolation, for instance:

$$\begin{aligned}
u_{i-\frac{1}{2},j+1,k} &= 2u_{i-\frac{1}{2},j,k} - u_{i-\frac{1}{2},j-1,k} \\
u_{i-\frac{1}{2},j,k+1} &= 2u_{i-\frac{1}{2},j,k} - u_{i-\frac{1}{2},j,k-1} \\
v_{i-1,j+\frac{1}{2},k} &= 2v_{i,j+\frac{1}{2},k} - v_{i+1,j+\frac{1}{2},k} \\
v_{i,j+\frac{1}{2},k+1} &= 2v_{i,j+\frac{1}{2},k} - v_{i,j+\frac{1}{2},k-1} \\
w_{i-1,j,k+\frac{1}{2}} &= 2w_{i,j,k+\frac{1}{2}} - w_{i+1,j,k+\frac{1}{2}} \\
w_{i,j+1,k+\frac{1}{2}} &= 2w_{i,j,k+\frac{1}{2}} - w_{i,j-1,k+\frac{1}{2}}.
\end{aligned} \tag{21}$$

According to [4, 7], the use of Eqs. (21) combined with the second order Runge-Kutta method to solve the Eq. (7) results in a method with good mass conservation properties when a large time step is used.

4 NUMERICAL RESULTS

This section, infludes a verification of the implemented methodology and a numerical study of the variation of the most influential parameters of the impact drop problem.

In this problem, we are interested in the temporal evolution of the three-dimensional shape of a drop that falls under gravity action from a distance H of a rigid wall. The parameters used in this study were: $L = diameter = 0.02$m, $U = 1$m/s and $g = -9.81$m/s^2 (resulting in $Fr = 2.26$). We consider a drop with an initial velocity of $w_0 = -1$m/s at a distance $H = 0.04$m from the center of the drop to the rigid wall.

Firstly, to verify the implementation of the code, we have simulated the problem using Newtonian and Oldroyd-B fluids at $Re = 5$. For the Oldroyd-B model, we used $Wi = 1$ and $\beta = 0.1$. Two meshes were adopted for the computations: $M1 : 60 \times 60 \times 50$ cells ($\delta h = 0.025$) and $M2 : 120 \times 120\times$ cells ($\delta h = 0.0125$). Figure 3 shows the comparison among our results and those presented by [9]. In addition, we have plotted in Fig. 3 results obtained by the OpenFOAM® CFD toolbox. The results obtained with the present methodology for two meshes show a good convergence with mesh refinement. Moreover, it is seen that in comparison with the other methods, our code produces satisfactory results, capturing the impact and spread of the drop.

As a further validation, Fig. 4 shows the time evolution of the distance of the drop until the rigid wall, where the analytical solution is defined by (no air resistance is assumed):

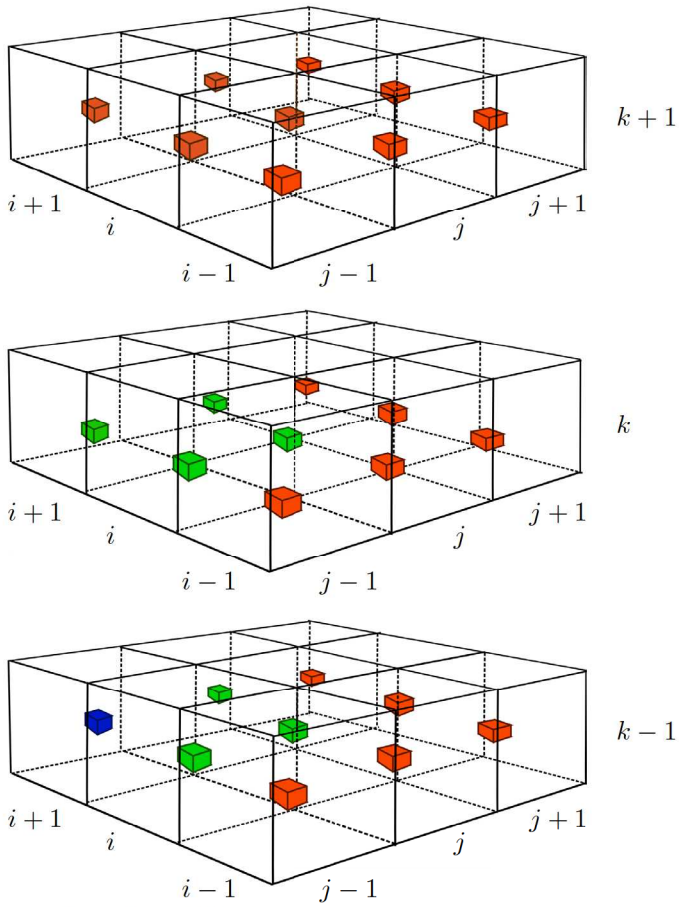

Figure 2: Illustration of three dimensional MAC cells for the normal vector given by $\mathbf{n} = \left(-\frac{\sqrt{3}}{3}, \frac{\sqrt{3}}{3}, \frac{\sqrt{3}}{3}\right)$: velocities are stored in the faces of each cell.

$$Height\ of\ drop\,(t) = \frac{g}{2}t^2 + w_0 t + H - \frac{diameter}{2}. \tag{22}$$

From Eq. (22) we can determine the time that the drop takes to reach the rigid wall, i.e., $t \approx 1.3272$. It is observed from Fig. 4 that our numerical scheme can predict very accurately the evolution of the height of the drop relative to rigid wall.

Based on the proposed method we simulate the impacting drop problem for various values of the non-dimensional parameters of Giesekus and XPP models.

Initially, we investigate the influence of β on the impacting drop problem for the Giesekus fluid. The data used for this simulation are: $Re = 5$, $Wi = 1$, $\alpha = 0.1$, $\gamma = 0.8$, $Q = 4$ and $Fr = 2.26$. Figure 5 illustrates the deformation history of the drop for varying β. When $\beta = 1$ the fluid becomes Newtonian while a value of β close to zero corresponds to more elastic fluids. It can be seen from Fig. 5 that as β decreases, the effect of the elasticity of the fluid increases leading to an overshoot in the width of the drop.

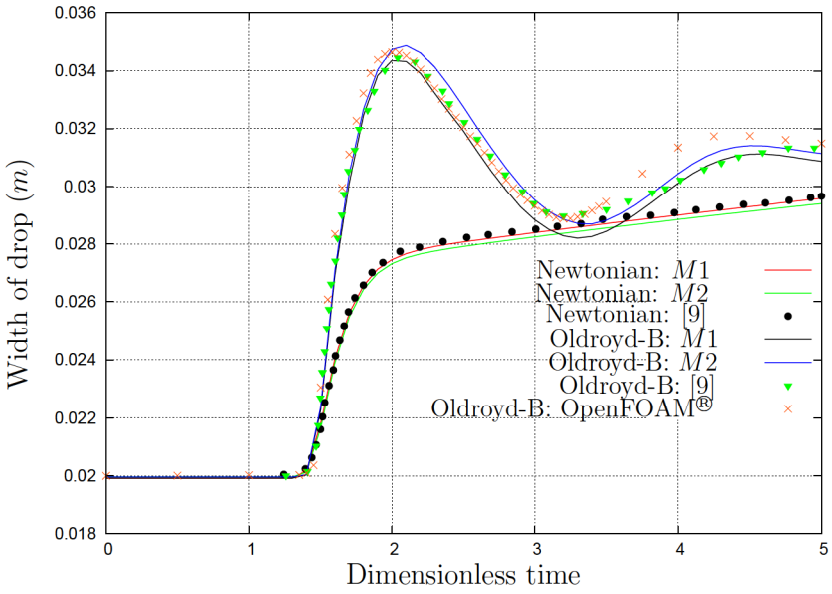

Figure 3: Numerical prediction of the time variation of the width of Newtonian and Oldroyd-B fluids at $Re = 5.0$ and $Fr = 2.26$.

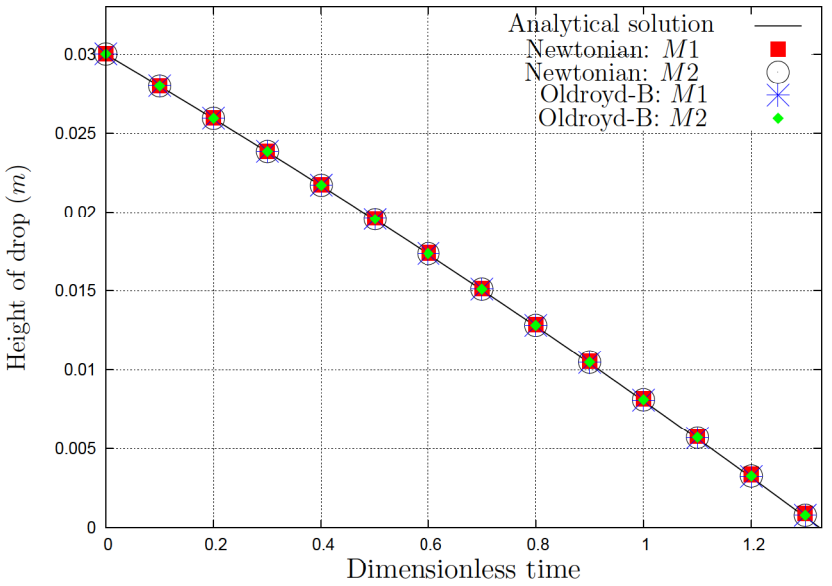

Figure 4: Numerical prediction of the height of drop with of Newtonian and Oldroyd-B fluids at $Re = 5$ and $Fr = 2.26$.

We also assessed the influence of the Reynolds number for a XPP fluid to investigate the effect of the viscosity in the drop shape. In this case, we adopted $Wi = 1$, $\beta = 0.2$, $\alpha = 0.1$, $\gamma = 0.8$, $Q = 4$ and $Fr = 2.26$. Figure 6 shows the time evolution of the drop

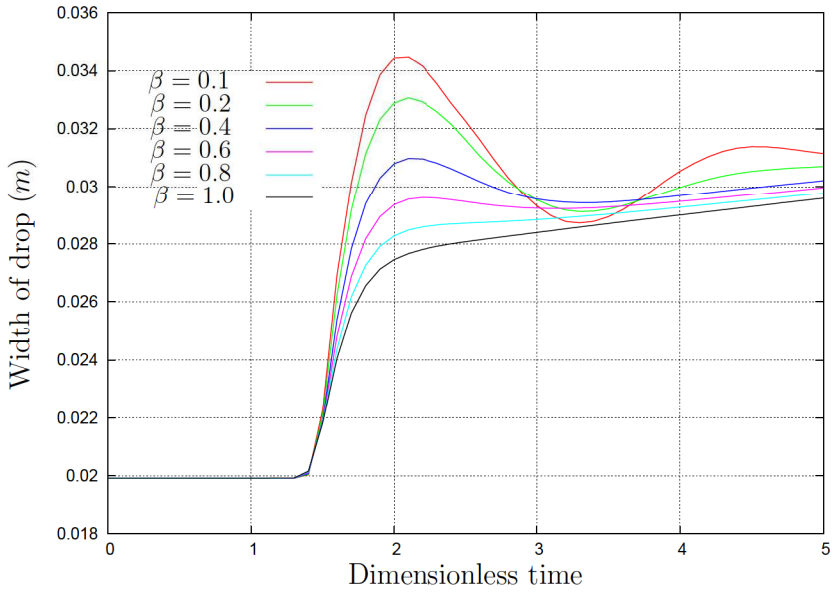

Figure 5: Influence of β in the numerical prediction of the drop width for the Giesekus fluid using $Re = 5$, $Wi = 1$, $\alpha = 0.1$ and $Fr = 2.26$.

width for different values of Re, illustrating that increasing the Reynolds number leads to a more spreading of the drop.

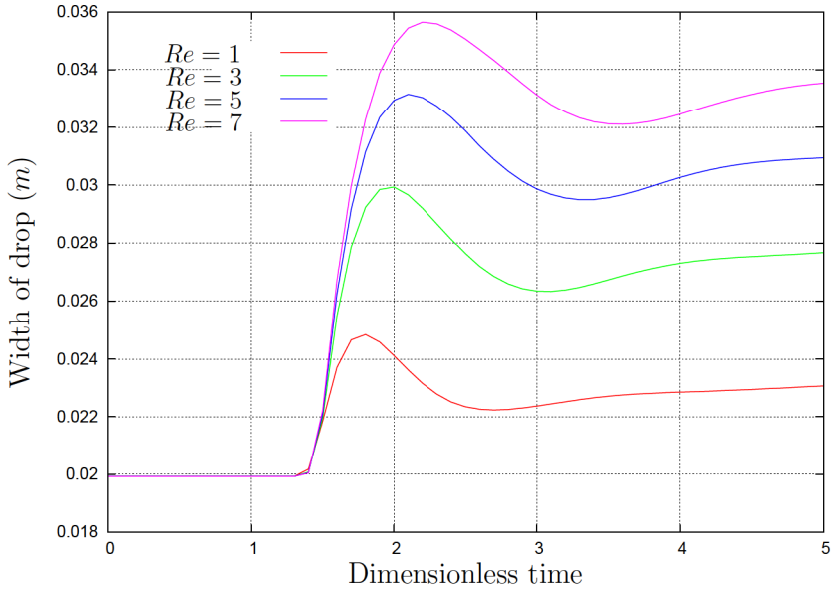

Figure 6: Influence of Re in the numerical prediction of the drop width for the XPP fluid using $Wi = 1$, $\beta = 0.2$, $\alpha = 0.1$, $\gamma = 0.8$, $Q = 4$ and $Fr = 2.26$.

We have also performed simulations to investigate the influence of gravity varying Fr

for a XPP fluid. Figure 7 shows that the width of the drop decreases with an increase of Fr.

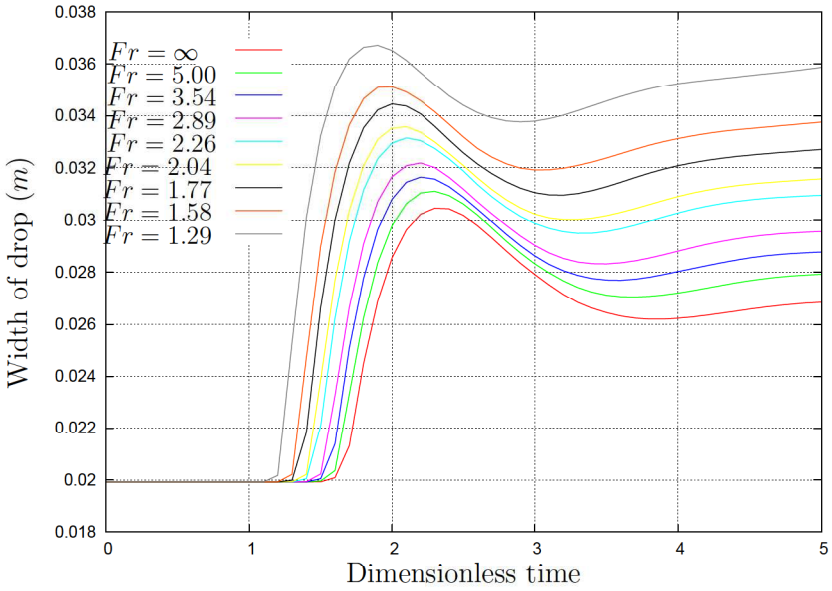

Figure 7: Influence of Fr in the numerical prediction of the drop width for a XPP fluid using $Re = 5$, $Wi = 1$, $\beta = 0.2$, $\alpha = 0.1$, $\gamma = 0.8$ and $Q = 4$.

Finally, we studied the influence of the Weissenberg number on the impacting problem of a XPP fluid drop. This parameter is related to the viscoelasticity of the fluid and according to Fig. 8, we note that increasing the Weissenberg number, leads to an increase of the width with a more efficient spreading due to the enhancement of shear thinning when Wi increases.

5 CONCLUSION

In this work we have presented a numerical investigation of the impacting drop problem for viscoelastic fluid flows. The code used in this study is a modification of the methodology proposed in [1]. In particular, in the context of the MAC method, an improvement in the interpolation of the marker particle velocities on the free surface is developed for the three-dimensions. The proposed methodology has been validated and compared with results from the literature. Finally, a study of the variation of the parameters of the Giesekus and XPP models for the impacting drop problem was performed for a wide range of the relevant dimensionless parameters.

6 ACKNOWLEDGMENTS

The authors acknowledge the financial support of the FAPESP (Fundação de Amparo à Pesquisa do Estado de São Paulo, Grants 2011/09194-7, 2013/07375-0 and the CNPq

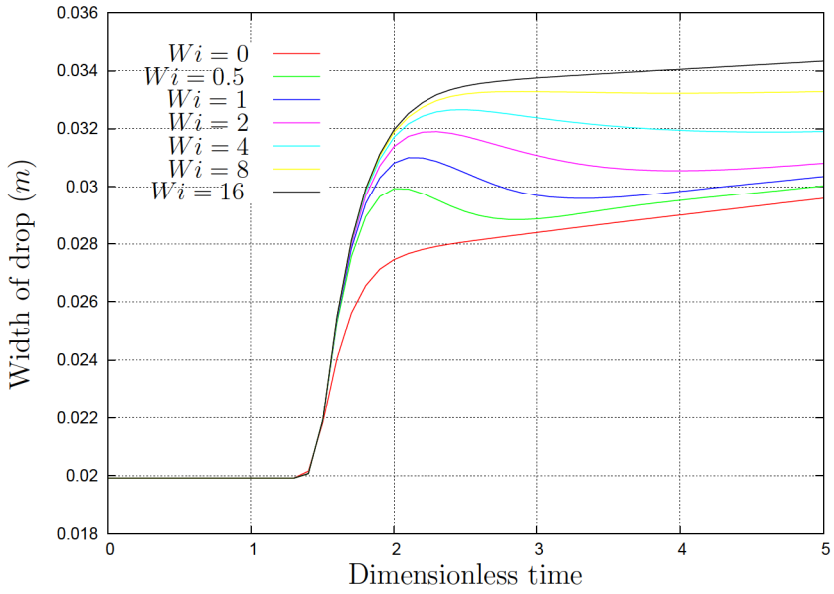

Figure 8: Influence of Wi in the numerical prediction of the drop width for the XPP fluid using $Re = 5$, $\beta = 0.4$, $\alpha = 0.1$, $\gamma = 0.8$, $Q = 4$ and $Fr = 2.26$.

(Conselho Nacional de Desenvolvimento Cientifico e Tecnologico), Grant 473589/2013-3.

REFERENCES

[1] R.A. Figueiredo, C.M. Oishi, J.A. Cuminato and M.A. Alves Three-dimensional transient complex free surface flows: Numerical simulation of XPP fluid, *Journal of Non-Newtonian Fluid Mechanics*, **195** (2013), 88 98.

[2] J.L. Favero, A.R. Secchi, N.S.M. Cardozo, and H. Jasak: Viscoelastic fluid analysis in internal and in free surface flows using the software OpenFOAM, *Computers & Chemical Engineering*, **34** (2010), 1984–1993.

[3] S.A. Roberts and R.R. Rao: Numerical simulations of mounding and submerging flows of shear-thinning jets impinging in a container, *Journal of Non-Newtonian Fluid Mechanics*, **166** (2011), 1100–1115.

[4] F.P. Martins, C.M. Oishi, F.S. Sousa and J.A. Cuminato: Numerical assessment of mass conservation on a MAC-type method for viscoelastic free surface flows, *6th European Congress on Computational Methods in Applied Sciences and Egineering*, **1** (2012), 6545–6562.

[5] A. Rafiee, M.T. Manzari and M. Hosseini: An incompressible SPH method for simulation of unsteady viscoelastic free-surface flows, *International Journal of Non-Linear Mechanics*, **42** (2007), 1210–1223.

[6] T. Jiang, J. Ouyang, B. Yang and J. Ren: The SPH method for simulating a viscoelastic drop impact and spreading on an inclined plate, *Computational Mechanics*, **45** (2010), 573–583.

[7] C.M. Oishi, F.P. Martins, M.F. Tomé and M.A. Alves: Numerical simulation of drop impact and jet buckling problems using the eXtended PomPom model, *Journal of Non-Newtonian Fluid Mechanics*, **169-170** (2012), 91–103.

[8] M.F. Tomé, L. Grossi, A. Castelo, J.A. Cuminato, N. Mangiavacchi, V.G. Ferreira, F.S. de Sousa and S. McKee: A numerical method for solving three-dimensional generalized Newtonian free surface flows, *Journal of Non-Newtonian Fluid Mechanics*, **123** (2004), 85–103.

[9] X. Xu, J. Ouyang, T. Jiang and Q. Li: Numerical simulation of 3D-unsteady viscoelastic free surface flows by improved smoothed particle hydrodynamics method, *Journal of Non-Newtonian Fluid Mechanics*, **177-178** (2012), 109–120.

[10] M.G.H.M. Baltussen, W.M.H. Verbeeten, A.C.B Bogaerds, M.A. Hulsen and G.W.M. Peters: Anisotropy parameter restrictions for the eXtended Pom-Pom model, *Journal of Non-Newtonian Fluid Mechanics*, **165** (2010), 1047–1054.

[11] L. Ville, L. Silva and T. Coupez: Convected level set method for the numerical simulation of fluid buckling, *International Journal for Numerical Methods in Fluids*, **66** (2011), 324–344.

[12] F. Habla, H. Marschall, O. Hinrichsen, L. Dietsche, H. Jasak, J.L. Favero: Numerical simulation of viscoelastic two-phase flows using openFOAM, *Chemical Engineering Science*, **66** (2011), 5487–5496.

[13] A.A. Amsden and F.H. Harlow: A simplified MAC technique for incompressible fluid flow calculations, *Journal of Computational Physics*, **6.2** (1970), 322–325.

[14] S. Mckee, M.F. Tomé, V.G. Ferreira, J.A. Cuminato, A. Castelo, F.S. Sousa and N. Mangiavacchi: The MAC method, *Computers & Fluids*, **37** (2008), 907–930.